

This is the accepted manuscript made available via CHORUS. The article has been published as:

Strong increase in ultrasound attenuation below μ_{c}/T in $\text{Sr}_{2-\text{RuO}_4}$: Possible evidence for domains

Sayak Ghosh, Thomas G. Kiely, Arkady Shekhter, F. Jerzembeck, N. Kikugawa, Dmitry A. Sokolov, A. P. Mackenzie, and B. J. Ramshaw

Phys. Rev. B **106**, 024520 — Published 27 July 2022

DOI: [10.1103/PhysRevB.106.024520](https://doi.org/10.1103/PhysRevB.106.024520)

Strong Increase in Ultrasound Attenuation Below T_c in Sr_2RuO_4 : Possible Evidence for Domains

Sayak Ghosh,¹ Thomas G. Kiely,¹ Arkady Shekhter,² F. Jerzembeck,³ N. Kikugawa,⁴ Dmitry A. Sokolov,³ A. P. Mackenzie,^{3,5} and B. J. Ramshaw^{1,*}

¹*Laboratory of Atomic and Solid State Physics, Cornell University, Ithaca, NY 14853, USA*

²*National High Magnetic Field Laboratory, Florida State University, Tallahassee, FL 32310, USA*

³*Max Planck Institute for Chemical Physics of Solids, Dresden, Germany*

⁴*National Institute for Materials Science, Tsukuba, Ibaraki 305-0003, Japan*

⁵*SUPA, School of Physics and Astronomy, University of St Andrews, North Haugh, St Andrews KY16 9SS, UK*

(Dated: July 13, 2022)

Recent experiments suggest that Sr_2RuO_4 has a two-component superconducting order parameter (OP). A two-component OP has multiple degrees of freedom in the superconducting state that can result in low-energy collective modes or the formation of domain walls—a possibility that would explain a number of experimental observations including the smallness of the signature of time reversal symmetry breaking at T_c and telegraph noise in critical current experiments. We use resonant ultrasound spectroscopy (RUS) to perform ultrasound attenuation measurements across the superconducting T_c of Sr_2RuO_4 . We find that compressional sound attenuation increases by a factor of seven immediately below T_c , in sharp contrast with what is found in both conventional (s -wave) and high- T_c (d -wave) superconductors. Our observations are most consistent with the presence of domain walls that separate different configurations of the superconducting OP. The fact that we only observe an increase in sound attenuation for compressional strains, and not for shear strains, suggests an inhomogeneous superconducting state formed of two distinct, accidentally-degenerate superconducting OPs that are not related to each other by symmetry. Whatever the mechanism, a factor of seven increase in sound attenuation is a singular characteristic that must be reconciled with any potential theory of superconductivity in Sr_2RuO_4 .

INTRODUCTION

One firm, if perhaps counter-intuitive, prediction of Bardeen, Cooper, and Schrieffer (BCS) theory is the contrasting behavior of the nuclear spin-lattice relaxation rate, $1/T_1$, and the ultrasonic attenuation, α [1]. One might expect both $1/T_1$ and α to decrease upon cooling from the normal state to the superconducting (SC) state as both processes involve the scattering of normal quasiparticles. In the SC state, however, Cooper pairing produces quantum coherence between quasiparticles of opposite spin and momentum. These correlations produce “coherence factors” that add constructively for nuclear relaxation and produce a peak—the Hebel-Slichter peak—in $1/T_1$ immediately below T_c [2]. In contrast, the coherence factors add destructively for sound attenuation and there is an immediate drop in α below T_c [3]. These experiments provided some of the strongest early evidence for the validity of BCS theory [1], and the drop in sound attenuation below T_c was subsequently confirmed in many elemental superconductors [4–7].

It came as a surprise, then, when peaks in the sound attenuation were discovered below T_c in two heavy-fermion superconductors: UPt_3 and URu_2Si_2 [8–10]. Specifically, peaks were observed in the longitudinal sound attenuation—when the sound propagation vector \mathbf{q} is parallel to the sound polarization \mathbf{u} : ($\mathbf{q} \parallel \mathbf{u}$). Transverse sound attenuation ($\mathbf{q} \perp \mathbf{u}$), on the other hand,

showed no peak below T_c but instead decreased with power law dependencies on T that were ultimately understood in terms of the presence of nodes in the SC gap [11]. Various theoretical proposals were put forward to understand the peaks in the longitudinal sound attenuation, including collective modes, domain-wall friction, and coherence-factors [12–15], but the particular mechanisms for UPt_3 and URu_2Si_2 were never pinned down (see Sigrist and Ueda [16] for a review). What is clear, however, is that a peak in sound attenuation below T_c is not a prediction of BCS theory and surely indicates unconventional superconductivity.

The superconductivity of Sr_2RuO_4 has many unconventional aspects, including time reversal symmetry (TRS) breaking [17–19], the presence of nodal quasiparticles [20–22], and a two-component SC OP [23, 24]. These observations have led to various recent theoretical proposals for the SC OP [25–31], requiring further experimental inputs to differentiate between them. Not only should the coherence factors differ for Sr_2RuO_4 compared to the s -wave BCS case, but there is the possibility of low-energy collective modes [32, 33] and domain-wall motion [34], all of which could be observable in the ultrasonic attenuation when measured at appropriate frequencies.

Prior ultrasonic attenuation measurements on Sr_2RuO_4 reported a power-law temperature dependence of the transverse sound attenuation, interpreted as evidence for nodes in the gap [20], but found no other unconventional behavior. The ultrasound technique employed in these previous measurements, pulse-echo ultrasound, can measure a pure shear response in the

* bradramshaw@cornell.edu

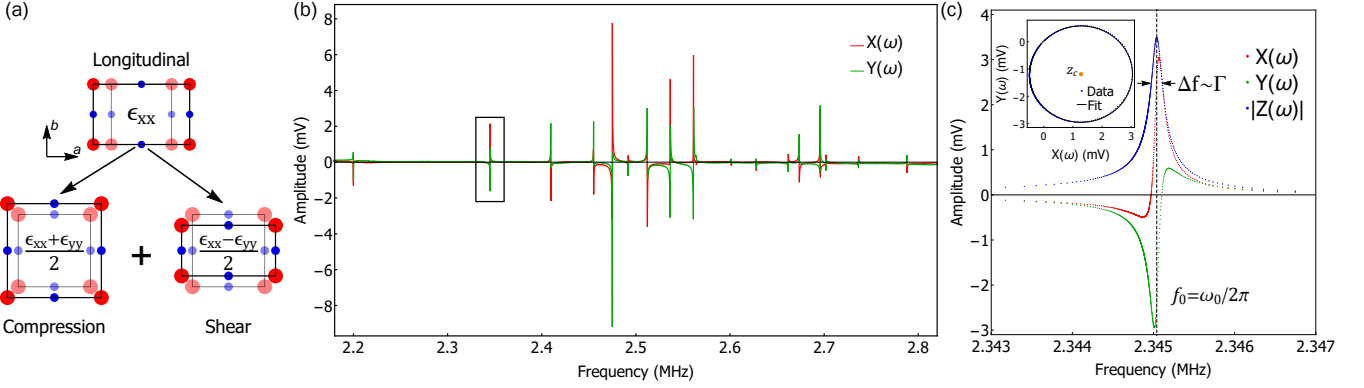


FIG. 1. **Measuring ultrasonic attenuation with resonant ultrasound spectroscopy.** (a) The Sr_2RuO_4 unit cell under a deformation corresponding to the longitudinal strain ϵ_{xx} , associated with the elastic constant c_{11} . This mode is a superposition of pure compression $\epsilon_{xx} + \epsilon_{yy}$ and pure shear $\epsilon_{xx} - \epsilon_{yy}$, associated with the elastic constants $(c_{11} + c_{12})/2$ and $(c_{11} - c_{12})/2$, respectively. (b) Resonant ultrasound spectrum of Sr_2RuO_4 between 2.2-2.8 MHz. $X(\omega)$ and $Y(\omega)$ are the real and the imaginary parts of the response. The boxed resonance is shown in detail in (c). (c) Zoom-in on the resonance near 2.34 MHz. The center of the resonance and the linewidth are indicated. Inset shows the same resonance plotted in complex plane and fit to a circle— z_c denotes the center of the circle.

transverse configuration but measures a combination of compression and shear response in the longitudinal configuration in a tetragonal crystal like Sr_2RuO_4 [35]. In particular, the L100 mode measures the elastic constant c_{11} , which is a mixture of pure compression, $(c_{11} + c_{12})/2$, and pure shear, $(c_{11} - c_{12})/2$ (see Figure 1(a)). Shear and compression strains couple to physical processes in fundamentally different ways and thus effects that couple exclusively to compressional sound may have been missed in previous measurements. In addition, pulse-echo operates at frequencies of order 100 MHz and higher, which may be too high in frequency—or too short in wavelength—to observe certain dynamical processes associated with large-scale correlations in the system. Thus, attenuation measurements that can separate the compression and shear responses, as well as measure at lower frequencies, may reveal features of the superconducting state in Sr_2RuO_4 not observed in previous experiments.

EXPERIMENT

We have measured the ultrasound attenuation of Sr_2RuO_4 across T_c using resonant ultrasound spectroscopy (RUS). RUS allows us to obtain the attenuation in all the independent symmetry channels in a single experiment (i.e. for all 5 symmetry components of strain in Sr_2RuO_4), and operates at frequencies of order 1 MHz. The sample space in our RUS apparatus requires exchange gas in order to thermalize the sample, preventing us from measuring below 1.25 K: see Ghosh *et al.* [23] for details of our custom-built, low-temperature RUS apparatus and the Supplemental Material [36] for details on the lock-in technique [37] used to measure the spectra.

The high-quality Sr_2RuO_4 crystal used in this experi-

ment was grown by the floating zone method—more details about the sample growth can be found in Bobowski *et al.* [38]. A single crystal was precision-cut along the [110], $[\bar{1}\bar{1}0]$ and [001] directions and polished to the dimensions $1.50 \text{ mm} \times 1.60 \text{ mm} \times 1.44 \text{ mm}$, with 1.44 mm along the tetragonal c axis. The sample quality was characterized by heat capacity and AC susceptibility measurements, as reported in Ghosh *et al.* [23]. The SC T_c measured by these techniques—approximately 1.43 K—agrees well with the T_c seen in our RUS experiment, indicating that the sample underwent uniform cooling during the experiment.

RUS measures the mechanical resonances of a three-dimensional solid. The frequencies of these resonances depend on the elastic moduli, density, and geometry of the sample, while the widths of these resonances are determined by the ultrasonic attenuation [39, 40]. Because each resonance mode is a superposition of multiple kinds of strain, the attenuation in all strain channels can be extracted by measuring a sufficient number of resonances—typically 2 or 3 times the number of unique strains (of which there are 5 for Sr_2RuO_4).

A segment of a typical RUS spectrum from our experiment is shown in Figure 1(b) (see the Supplemental Material [36] for the full spectrum). Each resonance can be modeled as the response $Z(\omega)$ of a damped harmonic oscillator driven at frequency ω (see Figure 1(c)),

$$Z(\omega) = X(\omega) + iY(\omega) = Ae^{i\phi}/[(\omega - \omega_0) + i\Gamma/2], \quad (1)$$

where X and Y are the real and imaginary parts of the response, and A , Γ , and ϕ are the amplitude, linewidth, and phase, respectively. The real and imaginary parts of the response form a circle in the complex plane. The response is measured at a set of frequencies that space the data points evenly around this circle: this is the most efficient way to precisely determine the resonant frequency

ω_0 and the linewidth Γ in a finite time (see Shekhter *et al.* [41] for details of the fitting procedure). We plot the temperature dependence of the linewidth for all our resonances measured through T_c in the S. For comparison, the attenuation α measured in conventional pulse-echo ultrasound is related to the resonance linewidth via $\alpha = \Gamma/v$, where v is the sound velocity (see the Supplemental Material [36] for a simple derivation).

RESULTS

When the sound wavelength, $\lambda = \frac{2\pi}{q}$, is much longer than the electronic mean free path l , i.e. when $ql \ll 1$, the electron-phonon system is said to be in the ‘hydrodynamic’ limit [42] (this is different than the hydrodynamic limit of electron transport). Given that the best Sr_2RuO_4 has a mean free path that is at most of order a couple of microns, and that our experimental wavelengths are of the order of 1 mm, we are well within the hydrodynamic limit. In this regime, we can express the linewidth Γ of a resonance ω_0 as

$$\frac{\Gamma}{\omega_0^2} = \sum_j \alpha_j \frac{\eta_j}{c_j}, \quad (2)$$

where c_j and η_j are the independent components of the elastic and viscosity tensors, respectively (see the Supplemental Material [36] for a derivation of Equation 2). Note that c_j and η_j can also be understood as the real and imaginary parts, respectively, of the full, dynamic elastic tensor. The coefficients α_j define the composition of a resonance, with $\alpha_j = \partial(\ln \omega_0^2)/\partial(\ln c_j)$ and $\sum_j \alpha_j = 1$ [39].

We measured the linewidths of 18 resonances and resolved them into the independent components of the viscosity tensor. Because viscosity depends only weakly on frequency in a Fermi liquid, and because Sr_2RuO_4 is a good Fermi liquid at low temperatures (just above T_c) [43], we can directly compare our measured viscosities to those made at much higher frequencies by pulse-echo ultrasound. These comparisons are made below, with further discussion in the Supplemental Material [36]. The tetragonal symmetry of Sr_2RuO_4 dictates that there are only six independent viscosity components, arising from the five irreducible representations (irreps) of strain in D_{4h} plus one component arising from coupling between the two distinct compression strains [23]. The six symmetry-resolved components of viscosity in Sr_2RuO_4 are plotted in Figure 2.

The shear viscosity $(\eta_{11} - \eta_{12})/2$ decreases below T_c in a manner similar to what is observed in conventional superconductors [3, 4]. We find that $(\eta_{11} - \eta_{12})/2$ is much larger than the other two shear viscosities, which is consistent with previous pulse-echo ultrasound experiments [20, 44]. On converting attenuation to viscosity, we find very good agreement between the resonant ultrasound and pulse-echo measurements of $(\eta_{11} - \eta_{12})/2$. This

is non-trivial because the bare sound attenuation—before conversion to viscosity—is two orders of magnitude larger in the pulse-echo experiments than in the RUS experiments. The much larger magnitude of $(\eta_{11} - \eta_{12})/2$, in comparison to η_{66} , may be due to the fact that the $\epsilon_{xx} - \epsilon_{yy}$ strain is associated with pushing the γ Fermi surface pocket toward the van Hove singularity [45]. The small values of η_{44} and η_{66} are comparable to the experimental background and any changes at T_c are too small to resolve at these low frequencies (see the Supplemental Material [36] for a discussion of the intrinsic and extrinsic contributions [46] to this background).

In contrast to the rather conventional shear viscosities, the three compressional viscosities each exhibit a strong increase below T_c . For in-plane compression—the strain that should couple strongest to the largely two-dimensional superconductivity of Sr_2RuO_4 —this increase is more than a factor of seven. The viscosity slowly decreases as the temperature is lowered after peaking just below T_c . The large increase in compression viscosity below T_c was not observed in previous longitudinal sound attenuation measurements made by pulse-echo ultrasound [20, 44]. There are two likely explanations for this. First, the L100 mode measured in pulse echo experiments measures η_{11} , which should be thought of as a mixture of the shear viscosity $(\eta_{11} - \eta_{12})/2$ and the compression viscosity $(\eta_{11} + \eta_{12})/2$ (Figure 1(a)). Because $(\eta_{11} - \eta_{12})/2$ is an order of magnitude larger than $(\eta_{11} + \eta_{12})/2$, the shear viscosity completely dominates the signal (see the Supplemental Material [36] for a comparison of η_{11} from RUS and pulse-echo experiments). Second, the pulse-echo experiments are conducted at frequencies that are two orders of magnitude higher than in the RUS experiments. The difference in time scales between the ultrasound and the dynamics system is critical because sound attenuation is intrinsically a dynamical quantity, thus the two techniques operating at different frequencies can observe different phenomena—we will return to this idea later on in the discussion.

ANALYSIS

We consider three possible mechanisms that could give rise to such an increase in sound attenuation below T_c . First, we calculate sound attenuation within a BCS-like framework that accounts for the differences in coherence factors that occur for various unconventional SC OPs. We find that a peak can indeed arise under certain circumstances but not under our experimental conditions. Second, we consider phonon-induced Cooper pair breaking in the SC state. This mechanism does lead to a sound attenuation peak just below T_c but it is inaccessibly narrow in our experiment. Finally, we show that a simple model of sound attenuation due to the formation of SC domains best matches the experimental data.

First, we calculate the change in sound attenuation due to coherent quasiparticle scattering in the SC state.

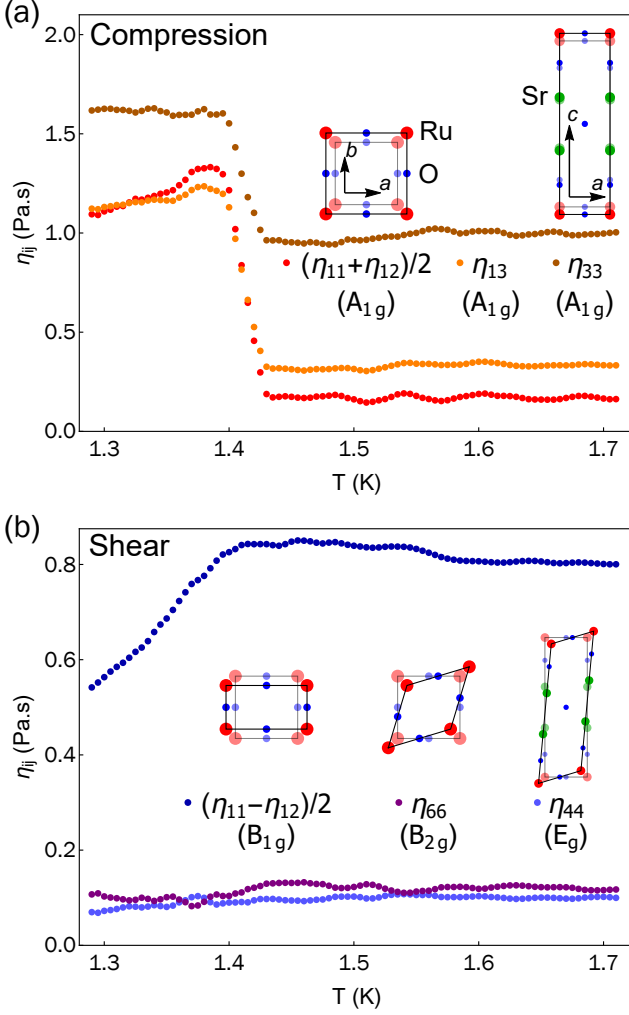


FIG. 2. **Symmetry-resolved sound viscosity in Sr_2RuO_4 .** (a) Compressional and (b) shear viscosities through T_c . The irreducible strain corresponding to each viscosity is shown— η_{13} arises due to coupling between the two A_{1g} strains. The compressional viscosities increase immediately below T_c , whereas no such features are observed in the shear viscosities.

The coherent scattering of Bogoliubov quasiparticles off of phonons results in suppressed sound attenuation below T_c in an s -wave superconductor [1]. In general, however, the coherence factors depend on the structure of the superconducting OP, motivating the idea that an unconventional superconducting OP might produce a peak in the sound attenuation below T_c . We find that a $d_{x^2-y^2}$ gap cannot not produce a peak in sound attenuation below T_c (Figure 3(a), see the Supplemental Material [36] for details of the calculation). For a TRS breaking gap, such as $p_x + ip_y$ or $d_{xz} + id_{yz}$, a Hebel-Slichter-like peak can appear below T_c if sufficiently large-angle scattering is allowed, but this scattering is only accessible at frequencies that are orders of magnitude higher than what is used in our experiment (Figure 3(b)). Hence we rule

out coherent scattering as the mechanism of increased attenuation below T_c .

Next we consider phonon-induced Cooper pair breaking as a mechanism for increased attenuation, similar to what is found below T_c in superfluid $^3\text{He-B}$ [47]. Pair-breaking in BCS superconductors requires a minimum energy of $2\Delta_0$, where Δ_0 is the gap magnitude. While superconducting gaps are typically much larger than ultrasound frequencies—the maximum gap magnitude in Sr_2RuO_4 , for example, is $2\Delta \sim 0.65$ meV or approximately 1 THz [48]—the gap does go to zero at T_c and at the nodes of certain OPs. Our calculations show that ultrasound frequencies of order ~ 10 GHz are required to produce an experimentally discernible peak with a $d_{x^2-y^2}$ gap (Figure 3(c)). At our experimental frequencies, the peak is only visible within 0.01 nK of T_c . For a fully gapped superconductor, like the TRS breaking state $p_x + ip_y$, the peak is suppressed even further. This clearly rules out pair breaking as the origin of the increased sound attenuation.

Finally, we consider the formation of domain walls in the superconducting state. Domain walls separate regions of degenerate OP configurations, such as $p_x + ip_y$ and $p_x - ip_y$, and can extract energy from sound waves by oscillating about their equilibrium positions [14]. Sigrist and Ueda [16] derive an expression for how domain wall motion leads to enhanced sound attenuation, which we write in the form

$$\eta(\omega, T) = A \frac{\rho_s^2}{\omega^2 + \omega_{DW}^2}, \quad (3)$$

where ρ_s is the superfluid density (proportional to the square of the superconducting gap), ω is the angular frequency of the sound wave, ω_{DW} is the lowest vibrational frequency of the domain wall, and all microscopic parameters have been subsumed into the coefficient A (see the Supplemental Material [36] for details of the parameters included in A). Near T_c , ρ_s and ω_{DW} can be expanded within a Ginzburg-Landau (GL) formalism as $\rho_s \propto |T - T_c|$ and $\omega_{DW} \propto |T - T_c|^{3/2}$. This gives an explicit temperature dependence to Equation 3:

$$\eta(\omega, T) = A \frac{|T/T_c - 1|^2}{\omega^2 + \omega_1^2 |T/T_c - 1|^3}, \quad (4)$$

where ω_1 is ω_{DW} in the limit $T \rightarrow 0$.

We fit all three measured viscosities to Equation 4 and extract $\omega_1 = 500 \pm 25$ MHz (Figure 3(d)). As the temperature approaches T_c from below, the domain wall frequency decreases to zero, producing a peak in the attenuation when the ultrasound frequency is approximately equal to the domain wall frequency. Note that $\eta(\omega)$ becomes frequency dependent in the presence of domain walls, in contrast to the frequency-independent viscosity of the Fermi liquid state above T_c . We use the average experimental frequency $\omega = 2.5$ MHz to extract ω_1 . Although our analysis uses resonance frequencies spanning 1.7 to 3.2 MHz, the position of the peak in η changes by

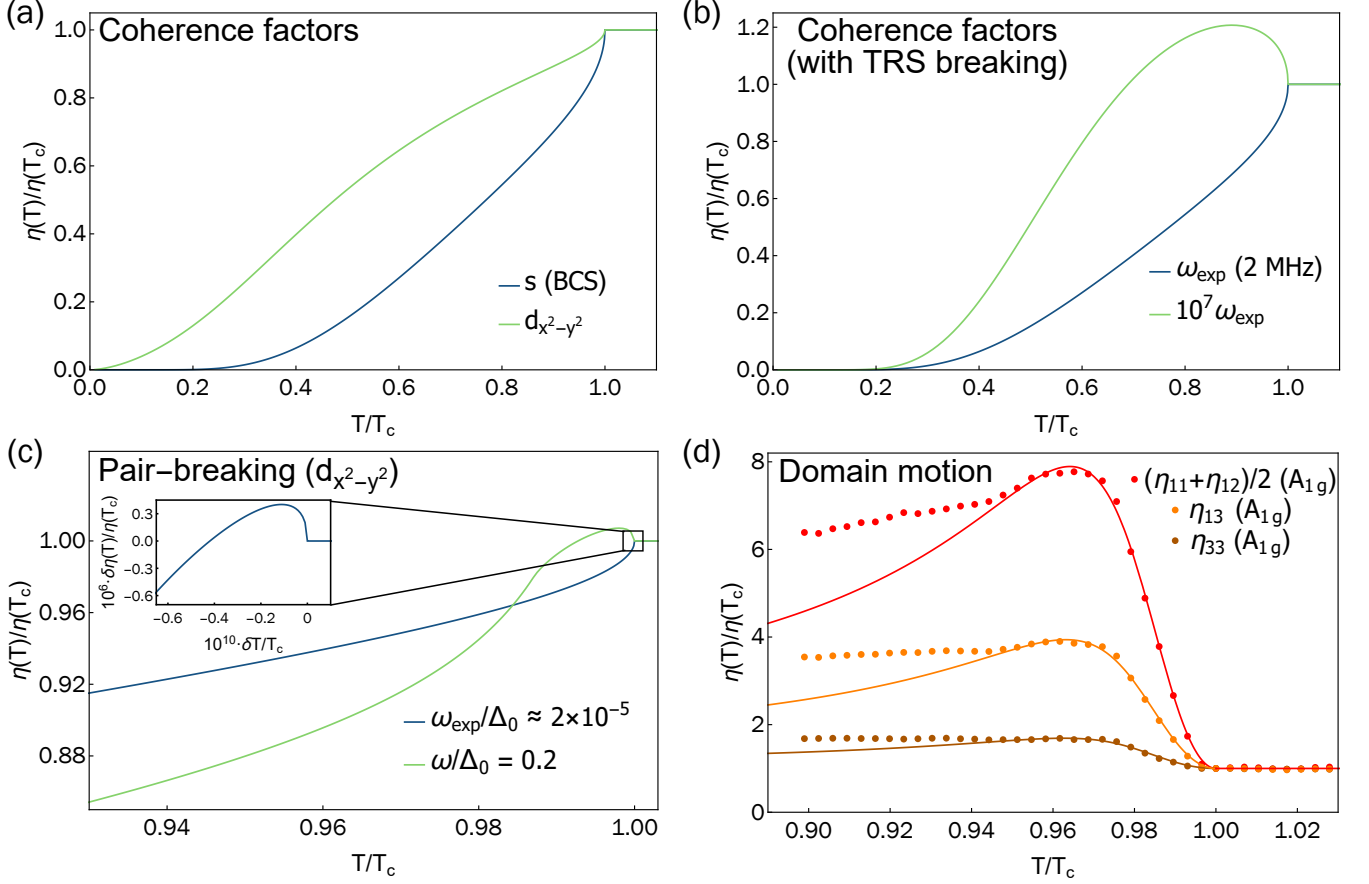


FIG. 3. **Comparison of different mechanisms for sound attenuation in the superconducting state.** (a) Normalized viscosity ($\eta(T)/\eta(T_c)$) for an isotropic s -wave gap and a $d_{x^2-y^2}$ gap, calculated within the BCS framework. (b) $\eta(T)/\eta(T_c)$ for a time reversal symmetry breaking gap below T_c . A peak is seen at high enough frequencies (\sim THz) but not at our experimental frequencies (\sim MHz). (c) Attenuation peak at different frequencies due to pair-breaking effects in a $d_{x^2-y^2}$ gap. The inset shows the plot at our experimental frequency in detail—a tiny peak is seen about 0.01 nK below T_c ($\delta\eta(T) = \eta(T) - \eta(T_c)$ and $\delta T = T - T_c$). (d) Normalized viscosity in the A_{1g} channels of Sr_2RuO_4 through T_c , fit to the viscosity expected from domain wall motion below T_c .

only about 14 mK over this frequency range, justifying our use of a single frequency for the fit (see the Supplemental Material [36] for plots at different frequencies).

The fit of Equation 4 deviates from the data for $T/T_c \lesssim 0.95$. This may be because of additional temperature dependencies, such as the temperature dependence of the domain wall frequency, that are not captured by the GL expansion, which is only valid near T_c [16]. Nevertheless, Equation 4 captures the correct shape of the rapid increase in attenuation below T_c in all three compression channels, using the same value of ω_1 for all three fits. The extracted frequency scale of $\omega_1 \approx 500$ MHz is also reasonable: studies of sound attenuation in nickel at MHz frequencies show similar magnitudes of increase in the magnetically ordered state when domains are present [49]. We note that the results of Josephson interferometry measurements have previously been interpreted as evidence for SC domains in Sr_2RuO_4 [19].

Previous pulse-echo ultrasound measurements, per-

formed at 83 MHz, did not identify any peak in η_{11} below T_c [20]. As we show in the Supplemental Material [36], the peak produced by Equation 3 becomes very broad at 83 MHz. Coupled with the fact that the temperature dependence of η_{11} is dominated by the strong temperature dependence of $(\eta_{11} - \eta_{12})/2$, it would be impossible to identify a peak below T_c at typical pulse-echo frequencies.

DISCUSSION

The factor of seven increase we find in the in-plane compressional viscosity is without precedent in a superconductor. For comparison, longitudinal attenuation increases by 50% below T_c in UPt_3 [10], and by a bit more than a factor of two in UBe_{13} [9]. There is also a qualitative difference between the increase in Sr_2RuO_4 and the increase seen in the heavy fermion superconductors:

the attenuation peaks sharply below T_c in both UPt₃ and UBe₁₃, with a peak width of approximately 10% of T_c . The compressional attenuation in Sr₂RuO₄, by contrast, decreases by only about 10% over the same relative temperature range. This suggests that something highly unconventional occurs in the SC state of Sr₂RuO₄, leading to a large increase in sound attenuation that is not confined to temperatures near T_c . The mechanism we find most consistent with the data is domain wall motion.

Assuming that we have established the likely origin of the increase in sound attenuation, we consider its implications for the superconductivity of Sr₂RuO₄. The formation of domains requires a two-component OP, either symmetry-enforced or accidental, reaffirming the conclusions of recent ultrasound studies of the elastic moduli and the sound velocity [23, 24].

We can learn more about which particular OPs are consistent with our experiment by considering which symmetry channels show an increase in attenuation. Domains attenuate ultrasound when the application of strain raises or lowers the condensation energy of one domain in comparison to a neighboring domain. A simple example is the “nematic” superconducting state proposed by Benhabib *et al.* [24], which is a d -wave OP of the E_g representation, transforming as $\{d_{xz}, d_{yz}\}$. Under $(\epsilon_{xx} - \epsilon_{yy})$ strain, domains of the d_{xz} configuration will be favored over the d_{yz} configuration (depending on the sign of the strain). This will cause some domains to grow and others to shrink, attenuating sound through the mechanism proposed by Sigrist and Ueda [16]. We find no increase in $(\eta_{11} - \eta_{12})/2$ below T_c , suggesting that a $\{d_{xz}, d_{yz}\}$ OP cannot explain the increase in compressional sound attenuation.

More generally, the lack of increase in attenuation in any of the shear channels implies that the SC state of Sr₂RuO₄ does not break rotational symmetry. Domains that are related to each other by time reversal symmetry can also be ruled out: there is no strain that can lift the degeneracy between, for example, a $p_x + ip_y$ domain and a $p_x - ip_y$ domain. The observed increase in sound attenuation under compressional strain is therefore quite unusual: as Sigrist and Ueda [16] point out, compressional strains can never lift the degeneracy between domains that are related by *any* symmetry, since compressional strains do not break the point group symmetry

of the lattice. Instead, attenuation in the compressional channel requires domains that couple differently to compressional strain, which in turn requires domains that are accidentally degenerate. Examples that are consistent with both NMR [50] and ultrasound [23, 24] include $\{d_{x^2-y^2}, g_{xy(x^2-y^2)}\}$ [30, 31, 51] and $\{s, d_{xy}\}$ [52]. Then, for example, domains of $d_{x^2-y^2}$ will couple differently to compressional strain than domains of $g_{xy(x^2-y^2)}$, leading to the growth of one domain type and an increase in compressional sound attenuation below T_c . Shear strain, meanwhile, does not change the condensation energy of any single-component OP (e.g. s , d_{xy} , $d_{x^2-y^2}$, or $g_{xy(x^2-y^2)}$) to first order in strain, which means that the lack of increase in shear attenuation below T_c is also consistent with an accidentally-degenerate OP. This is also consistent with the lack of a cusp in T_c under applied shear strain [53, 54].

Recent theoretical work [34] has shown that domain walls between $d_{x^2-y^2}$ and $g_{xy(x^2-y^2)}$ OPs may provide an explanation of the observation of half-quantum vortices in Sr₂RuO₄ *without* a spin-triplet OP [55]—a result that is otherwise inconsistent with the singlet pairing suggested by NMR [50]. Willa *et al.* [31], followed by Yuan *et al.* [34], have shown that domains between such states stabilize a TRS-breaking $d_{x^2-y^2} \pm ig_{xy(x^2-y^2)}$ state near the domain wall. This would naturally explain why probes of TRS breaking, such as the Kerr effect and μ SR [18, 56], see such a small effect at T_c in Sr₂RuO₄.

One significant challenge for the two-component OP scenario is that, whether accidentally degenerate or not, a two component OP should generically produce two superconducting T_c s. The lack of a heat capacity signature from an expected second transition under uniaxial strain [57] can only be explained if the second, TRS-breaking transition is particularly weak—a result that might be consistent with the TRS-breaking state appearing only along domain walls. Finally, it is worth noting that there are other mechanisms of ultrasonic attenuation that we have not explored here, including collective modes and gapless excitations such as edge currents that might appear along domain walls even if the domains are related by symmetry. Future ultrasound experiments under applied static strain and magnetic fields are warranted as certain types of domain walls can couple to these fields, thereby affecting the sound attenuation through T_c .

-
- [1] J. Bardeen, L. N. Cooper, and J. R. Schrieffer, Theory of superconductivity, Phys. Rev. **108**, 1175 (1957).
 - [2] L. C. Hebel and C. P. Slichter, Nuclear relaxation in superconducting aluminum, Phys. Rev. **107**, 901 (1957).
 - [3] R. W. Morse, T. Olsen, and J. D. Gavenda, Evidence for anisotropy of the superconducting energy gap from ultrasonic attenuation, Phys. Rev. Lett. **3**, 15 (1959).
 - [4] M. Levy, Ultrasonic attenuation in superconductors for $ql < 1$, Phys. Rev. **131**, 1497 (1963).
 - [5] J. R. Leibowitz, Ultrasonic shear wave attenuation in su-

- perconducting tin, Phys. Rev. **133**, A84 (1964).
- [6] L. T. Claiborne and N. G. Einspruch, Energy-gap anisotropy in In-doped Sn, Phys. Rev. Lett. **15**, 862 (1965).
- [7] K. Fossheim, Electromagnetic shear-wave interaction in a superconductor, Phys. Rev. Lett. **19**, 344 (1967).
- [8] B. Batlogg, D. Bishop, B. Golding, C. M. Varma, Z. Fisk, J. L. Smith, and H. R. Ott, λ -shaped ultrasound-attenuation peak in superconducting (U,Th)Be₁₃, Phys. Rev. Lett. **55**, 1319 (1985).

- [9] B. Golding, D. J. Bishop, B. Batlogg, W. H. Haemmerle, Z. Fisk, J. L. Smith, and H. R. Ott, Observation of a collective mode in superconducting UBe_{13} , *Phys. Rev. Lett.* **55**, 2479 (1985).
- [10] V. Müller, D. Maurer, E. Scheidt, C. Roth, K. Lüders, E. Bucher, and H. Bömmel, Observation of a lambda-shaped ultrasonic attenuation peak in superconducting UPt_3 , *Solid State Communications* **57**, 319 (1986).
- [11] J. Moreno and P. Coleman, Ultrasound attenuation in gap-anisotropic systems, *Phys. Rev. B* **53**, R2995 (1996).
- [12] K. Miyake and C. M. Varma, Landau-Khalatnikov damping of ultrasound in heavy-fermion superconductors, *Phys. Rev. Lett.* **57**, 1627 (1986).
- [13] H. Monien, L. Tewordt, and K. Scharnberg, Ultrasound attenuation due to order parameter collective modes in impure anisotropic p-wave superconductors, *Solid State Communications* **63**, 1027 (1987).
- [14] R. Joynt, T. M. Rice, and K. Ueda, Acoustic attenuation due to domain walls in anisotropic superconductors, with application to $\text{U}_{1-x}\text{Th}_x\text{Be}_{13}$, *Phys. Rev. Lett.* **56**, 1412 (1986).
- [15] L. Coffey, Theory of ultrasonic attenuation in impure anisotropic p-wave superconductors, *Phys. Rev. B* **35**, 8440 (1987).
- [16] M. Sigrist and K. Ueda, Phenomenological theory of unconventional superconductivity, *Rev. Mod. Phys.* **63**, 239 (1991).
- [17] G. M. Luke, Y. Fudamoto, K. M. Kojima, M. I. Larkin, J. Merrin, B. Nachumi, Y. J. Uemura, Y. Maeno, Z. Q. Mao, Y. Mori, H. Nakamura, and M. Sigrist, Time-reversal symmetry-breaking superconductivity in Sr_2RuO_4 , *Nature* **394**, 558 (1998).
- [18] J. Xia, Y. Maeno, P. T. Beyersdorf, M. M. Fejer, and A. Kapitulnik, High resolution polar kerr effect measurements of Sr_2RuO_4 : Evidence for broken time-reversal symmetry in the superconducting state, *Phys. Rev. Lett.* **97**, 167002 (2006).
- [19] F. Kidwingira, J. D. Strand, D. J. Van Harlingen, and Y. Maeno, Dynamical superconducting order parameter domains in Sr_2RuO_4 , *Science* **314**, 1267 (2006).
- [20] C. Lupien, W. A. MacFarlane, C. Proust, L. Taillefer, Z. Q. Mao, and Y. Maeno, Ultrasound attenuation in Sr_2RuO_4 : An angle-resolved study of the superconducting gap function, *Phys. Rev. Lett.* **86**, 5986 (2001).
- [21] E. Hassinger, P. Bourgeois-Hope, H. Taniguchi, S. René de Cotret, G. Grissonnanche, M. S. Anwar, Y. Maeno, N. Doiron-Leyraud, and L. Taillefer, Vertical line nodes in the superconducting gap structure of Sr_2RuO_4 , *Phys. Rev. X* **7**, 011032 (2017).
- [22] R. Sharma, S. D. Edkins, Z. Wang, A. Kostin, C. Sow, Y. Maeno, A. P. Mackenzie, J. C. S. Davis, and V. Madhavan, Momentum-resolved superconducting energy gaps of Sr_2RuO_4 from quasiparticle interference imaging, *Proceedings of the National Academy of Sciences* **117**, 5222 (2020).
- [23] S. Ghosh, A. Shekhter, F. Jerzembeck, N. Kikugawa, D. A. Sokolov, M. Brando, A. P. Mackenzie, C. W. Hicks, and B. J. Ramshaw, Thermodynamic evidence for a two-component superconducting order parameter in Sr_2RuO_4 , *Nature Physics* **17**, 199 (2021).
- [24] S. Benhabib, C. Lupien, I. Paul, L. Berges, M. Dion, M. Nardone, A. Zitouni, Z. Q. Mao, Y. Maeno, A. Georges, L. Taillefer, and C. Proust, Ultrasound evidence for a two-component superconducting order parameter in Sr_2RuO_4 , *Nature Physics* **17**, 194 (2021).
- [25] A. Ramires and M. Sigrist, Superconducting order parameter of Sr_2RuO_4 : A microscopic perspective, *Phys. Rev. B* **100**, 104501 (2019).
- [26] A. T. Rømer, D. D. Scherer, I. M. Eremin, P. J. Hirschfeld, and B. M. Andersen, Knight shift and leading superconducting instability from spin fluctuations in Sr_2RuO_4 , *Phys. Rev. Lett.* **123**, 247001 (2019).
- [27] H. S. Røising, T. Scaffidi, F. Flicker, G. F. Lange, and S. H. Simon, Superconducting order of Sr_2RuO_4 from a three-dimensional microscopic model, *Phys. Rev. Research* **1**, 033108 (2019).
- [28] T. Scaffidi, Degeneracy between even- and odd-parity superconductivity in the quasi-1D Hubbard model and implications for Sr_2RuO_4 (2020), arXiv:2007.13769.
- [29] H. G. Suh, H. Menke, P. M. R. Brydon, C. Timm, A. Ramires, and D. F. Agterberg, Stabilizing even-parity chiral superconductivity in Sr_2RuO_4 , *Phys. Rev. Research* **2**, 032023 (2020).
- [30] S. A. Kivelson, A. C. Yuan, B. Ramshaw, and R. Thomale, A proposal for reconciling diverse experiments on the superconducting state in Sr_2RuO_4 , *npj Quantum Materials* **5**, 43 (2020).
- [31] R. Willa, M. Hecker, R. M. Fernandes, and J. Schmalian, Inhomogeneous time-reversal symmetry breaking in Sr_2RuO_4 , *Phys. Rev. B* **104**, 024511 (2021).
- [32] M. Sigrist, Ehrenfest Relations for Ultrasound Absorption in Sr_2RuO_4 , *Progress of Theoretical Physics* **107**, 917 (2002).
- [33] S. B. Chung, S. Raghu, A. Kapitulnik, and S. A. Kivelson, Charge and spin collective modes in a quasi-one-dimensional model of Sr_2RuO_4 , *Phys. Rev. B* **86**, 064525 (2012).
- [34] A. C. Yuan, E. Berg, and S. A. Kivelson, Strain-induced time reversal breaking and half quantum vortices near a putative superconducting tetracritical point in Sr_2RuO_4 , *Phys. Rev. B* **104**, 054518 (2021).
- [35] K. Brugger, Pure modes for elastic waves in crystals, *Journal of Applied Physics* **36**, 759 (1965).
- [36] See Supplemental Material at [URL will be inserted by publisher] for details of the RUS experiment and theoretical calculations of viscosity.
- [37] F. F. Balakirev, S. M. Ennaceur, R. J. Migliori, B. Maiorov, and A. Migliori, Resonant ultrasound spectroscopy: The essential toolbox, *Review of Scientific Instruments* **90**, 121401 (2019).
- [38] J. S. Bobowski, N. Kikugawa, T. Miyoshi, H. Suwa, H.-S. Xu, S. Yonezawa, D. A. Sokolov, A. P. Mackenzie, and Y. Maeno, Improved single-crystal growth of Sr_2RuO_4 , *Condensed Matter* **4** (2019).
- [39] B. J. Ramshaw, A. Shekhter, R. D. McDonald, J. B. Betts, J. N. Mitchell, P. H. Tobash, C. H. Mielke, E. D. Bauer, and A. Migliori, Avoided valence transition in a plutonium superconductor, *Proceedings of the National Academy of Sciences* **112**, 3285 (2015).
- [40] S. Ghosh, M. Matty, R. Baumbach, E. D. Bauer, K. A. Modic, A. Shekhter, J. A. Mydosh, E.-A. Kim, and B. J. Ramshaw, One-component order parameter in URu_2Si_2 uncovered by resonant ultrasound spectroscopy and machine learning, *Science Advances* **6** (2020).
- [41] A. Shekhter, B. J. Ramshaw, R. Liang, W. N. Hardy, D. A. Bonn, F. F. Balakirev, R. D. McDonald, J. B. Betts, S. C. Riggs, and A. Migliori, Bounding the pseudogap with a line of phase transitions in $\text{YBa}_2\text{Cu}_3\text{O}_{6+\delta}$,

- Nature **498**, 75 EP (2013).
- [42] F. S. Khan and P. B. Allen, Sound attenuation by electrons in metals, Phys. Rev. B **35**, 1002 (1987).
 - [43] D. Forsythe, S. R. Julian, C. Bergemann, E. Pugh, M. J. Steiner, P. L. Alireza, G. J. McMullan, F. Nakamura, R. K. W. Haselwimmer, I. R. Walker, S. S. Saxena, G. G. Lonzarich, A. P. Mackenzie, Z. Q. Mao, and Y. Maeno, Evolution of fermi-liquid interactions in Sr_2RuO_4 under pressure, Phys. Rev. Lett. **89**, 166402 (2002).
 - [44] C. Lupien, *Ultrasound attenuation in the unconventional superconductor Sr_2RuO_4* , Ph.D. thesis (2002).
 - [45] M. E. Barber, F. Lechermann, S. V. Streltsov, S. L. Skornyakov, S. Ghosh, B. J. Ramshaw, N. Kikugawa, D. A. Sokolov, A. P. Mackenzie, C. W. Hicks, and I. I. Mazin, Role of correlations in determining the van hove strain in Sr_2RuO_4 , Phys. Rev. B **100**, 245139 (2019).
 - [46] T. Christopoulos, O. Tsilipakos, G. Sinatkas, and E. E. Kriezis, On the calculation of the quality factor in contemporary photonic resonant structures, Opt. Express **27**, 14505 (2019).
 - [47] S. Adenwalla, Z. Zhao, J. B. Ketterson, and B. K. Sarma, Measurements of the pair-breaking edge in superfluid $^3\text{He}-B$, Phys. Rev. Lett. **63**, 1811 (1989).
 - [48] I. A. Firmo, S. Lederer, C. Lupien, A. P. Mackenzie, J. C. Davis, and S. A. Kivelson, Evidence from tunneling spectroscopy for a quasi-one-dimensional origin of superconductivity in Sr_2RuO_4 , Phys. Rev. B **88**, 134521 (2013).
 - [49] R. Leonard, A. Barone, R. Truell, C. Elbaum, and B. E. Noltingk, *Acoustics II* (Springer-Verlag, Berlin Heidelberg, 1962).
 - [50] A. Pustogow, Y. Luo, A. Chronister, Y.-S. Su, D. A. Sokolov, F. Jerzembeck, A. P. Mackenzie, C. W. Hicks, N. Kikugawa, S. Raghu, E. D. Bauer, and S. E. Brown, Constraints on the superconducting order parameter in Sr_2RuO_4 from oxygen-17 nuclear magnetic resonance, Nature **574**, 72 (2019).
 - [51] J. Clepkens, A. W. Lindquist, X. Liu, and H.-Y. Kee, Higher angular momentum pairings in interorbital shadowed-triplet superconductors: Application to Sr_2RuO_4 , Phys. Rev. B **104**, 104512 (2021).
 - [52] A. T. Rømer, P. J. Hirschfeld, and B. M. Andersen, Superconducting state of Sr_2RuO_4 in the presence of longer-range coulomb interactions, Phys. Rev. B **104**, 064507 (2021).
 - [53] C. W. Hicks, D. O. Brodsky, E. A. Yelland, A. S. Gibbs, J. A. N. Bruin, M. E. Barber, S. D. Edkins, K. Nishimura, S. Yonezawa, Y. Maeno, and A. P. Mackenzie, Strong increase of T_c of Sr_2RuO_4 under both tensile and compressive strain, Science **344**, 283 (2014).
 - [54] C. A. Watson, A. S. Gibbs, A. P. Mackenzie, C. W. Hicks, and K. A. Moler, Micron-scale measurements of low anisotropic strain response of local T_c in Sr_2RuO_4 , Phys. Rev. B **98**, 094521 (2018).
 - [55] J. Jang, D. G. Ferguson, V. Vakaryuk, R. Budakian, S. B. Chung, P. M. Goldbart, and Y. Maeno, Observation of half-height magnetization steps in Sr_2RuO_4 , Science **331**, 186 (2011).
 - [56] V. Grinenko, S. Ghosh, R. Sarkar, J.-C. Orain, A. Nikitin, M. Elender, D. Das, Z. Guguchia, F. Brückner, M. E. Barber, J. Park, N. Kikugawa, D. A. Sokolov, J. S. Bobowski, T. Miyoshi, Y. Maeno, A. P. Mackenzie, H. Luetkens, C. W. Hicks, and H.-H. Klauss, Split superconducting and time-reversal symmetry-breaking transitions in Sr_2RuO_4 under stress, Nature Physics **17**, 748 (2021).
 - [57] Y.-S. Li, N. Kikugawa, D. A. Sokolov, F. Jerzembeck, A. S. Gibbs, Y. Maeno, C. W. Hicks, J. Schmalian, M. Nicklas, and A. P. Mackenzie, High-sensitivity heat-capacity measurements on Sr_2RuO_4 under uniaxial pressure, Proceedings of the National Academy of Sciences **118** (2021).

ACKNOWLEDGMENTS

B. J. R. and S. G. acknowledge support for building the experiment, collecting and analyzing the data, and writing the manuscript from the Office of Basic Energy Sciences of the United States Department of Energy under award no. DE-SC0020143. B.J.R. and S.G. acknowledge support from the Cornell Center for Materials Research with funding from the Materials Research Science and Engineering Centers program of the National Science Foundation (cooperative agreement no. DMR-1719875). T. G. K. acknowledge support from the National Science Foundation under grant no. PHY-2110250. N. K. acknowledges support from Japan Society for the Promotion of Science (JSPS) KAKENHI (Nos. JP17H06136, JP18K04715, and 21H01033)) and Japan Science and Technology Agency Mirai Program (JPMJMI18A3) in Japan.